JACS
JOURNAL OF THE AMERICAN CHEMICAL SOCIETY
Communication
pubs.acs.org/JACS

Mechanistic Study of the Photochemical Hydroxide Ion Release from 9-Hydroxy-10-methyl-9-phenyl-9,10-dihydroacridine

Dapeng Zhou,[†] Renat Khatmullin,[†] Janitha Walpita,[†] Nicholas A. Miller,[†] Hoi Ling Luk,[‡] Shubham Vyas,[‡] Christopher M. Hadad,[‡] and Ksenija D. Glusac*[,†]

[†]Department of Chemistry, Bowling Green State University, Bowling Green, Ohio 43403, United States
[‡]Department of Chemistry and Biochemistry, The Ohio State University, Columbus, Ohio 43210, United States

Supporting Information

ABSTRACT: The excited-state behavior of 9-hydroxy-10-methyl-9-phenyl-9,10-dihydroacridine and its derivative, 9-methoxy-10-methyl-9-phenyl-9,10-dihydroacridine (AcrOR, R = H, Me), was studied via femtosecond and nanosecond UV−vis transient absorption spectroscopy. The solvent effects on C−O bond cleavage were clearly identified: a fast heterolytic cleavage (τ = 108 ps) was observed in protic solvents, while intersystem crossing was observed in aprotic solvents. Fast heterolysis generates 10-methyl-9-phenylacridinium (Acr^+) and ^-OH, which have a long recombination lifetime (no signal decay was observed within 100 μs). AcrOH exhibits the characteristic behavior needed for its utilization as a chromophore in the pOH jump experiment.

Photohydroxide emitters are a class of compounds that release hydroxide anions (^-OH) to induce a pOH jump upon UV−vis irradiation. This process is similar to the pH jump methods achieved using various photoacids.[1−4] The pOH jump is generally achieved through heterolytic cleavage of the C−O bond, as is exhibited by compounds such as 9-fluorenol,[5,6] 9-phenylxanthen-9-ol,[7] and triphenylmethane hydroxide,[8,9] whose resonance structures stabilize the resulting carbocations. The application of these compounds in driving a photochemical pOH jump is mostly limited by the fast recombination of hydroxide and the carbocation.[5−7] Additionally, homolytic C−O bond cleavage can complicate the chemistry with the formation of hydroxyl radical ($^•OH$).[5,7,10]

Malachite green carbinol base (MGCB) has been suitable for photochemical pOH jump experiments[9] because the lifetime of ^-OH, which is generated in 300 ps,[8] is several minutes, and $^•OH$ is not formed. Upon excitation, MGCB was found to induce a jump from pH 6 to 11, making it a possible agent for studies of conformational changes in DNA/RNA[11,12] and also for the release of drugs from host molecules.[13]

Recently, Fréchet and co-workers discovered that 9-hydroxy/methoxy-10-methyl-9-phenyl-9,10-dihydroacridine (AcrOR, R = H, Me) exhibits photochemical behavior somewhat similar to that of MGCB.[14] Upon irradiation in H_2O/acetonitrile (ACN) mixtures, AcrOH releases 10-methyl-9-phenylacridinium (Acr^+) and ^-OH, resulting in a pOH jump that lasts longer than that of MGCB. However, the photochemical mechanism of AcrOH has not been studied until now. This study presents a detailed investigation of the excited-state dynamics of AcrOR via femtosecond (fs) and nanosecond (ns) transient absorption (TA) spectroscopy (Scheme 1), including the varying solvent-facilitated pathways of Acr^+ generation. Generation of Acr^+ is obvious with protic solvation (methanol, MeOH), while an intersystem crossing (ISC) process is observed with aprotic solvation (ACN and benzene).

Scheme 1. Excited-State Behavior of AcrOH in Different Solvents: MeOH (blue) and ACN or Benzene (red)[a]

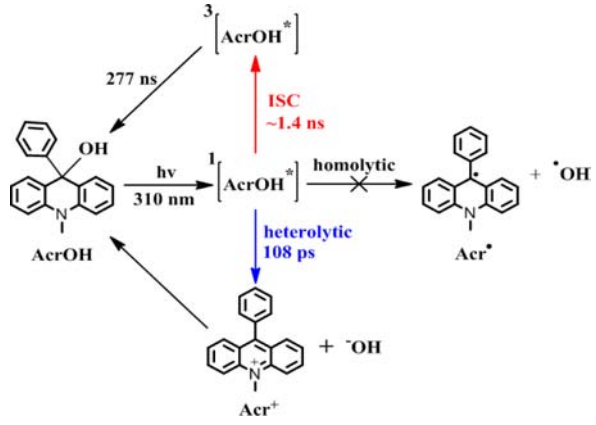

[a]For AcrOMe, τ_{hetero} = 83 ps and τ_{ISC} = ∼550 ps.

To evaluate the driving force for the excited-state heterolytic and homolytic C−O bond cleavage in AcrOH, a Förster energy diagram[15] was constructed from pH-dependent absorption and emission measurements along with the previously known reduction and oxidation potentials of Acr^+ and ^-OH (Figure S1 in the Supporting Information). From pH-dependent absorption measurements, the ground-state pseudobase pK_a value of AcrOH was determined to be 11.11, which is consistent with the literature.[16] On the basis of the Förster energy diagram, the driving forces for the excited-state hetero- and homolytic C−O bond cleavages were evaluated as $\Delta^1G^*_{hetero}$ = −1.048 eV, $\Delta^3G^*_{hetero}$ = −0.263 eV, $\Delta^1G^*_{homo}$ = −1.513, and $\Delta^3G^*_{homo}$ = −0.728 eV, indicating that both heterolytic and homolytic cleavage are possible in the excited state.

Received: April 2, 2012
Published: July 5, 2012

   dx.doi.org/10.1021/ja3031888 | J. Am. Chem. Soc. 2012, 134, 11301−11303

The geometry of the AcrOH ground state was optimized and the characters of the AcrOH excited states were evaluated using density functional theory (DFT) and time-dependent DFT calculations, respectively (Table S1 and Figure S2). The difference density plots[17,18] shown in Figure S2 indicate that the S_0-S_1 transition exhibits $\pi-\pi^*$ character within the acridine framework, while the S_0-S_2 transition generates a $\pi-\pi^*$ state in which an intramolecular electron transfer from the acridine framework to the phenyl moiety occurs. The laser measurements shown in this work were performed using a 310 nm excitation pulse; when compared to the calculated vertical excitations (Figure S2), this laser excitation should generate only the singlet excited (S_1) state with $\pi-\pi^*$ character.

The photochemical behavior of AcrOH in different solvents (ACN, benzene, and MeOH) was investigated using the fs TA technique. In ACN, the $t = 0$ TA spectrum of AcrOH exhibits a broad absorbance from 350 to 800 nm with λ_{max} at ~780 nm that decays with a lifetime of 1.4 ns (Figure 1). This component

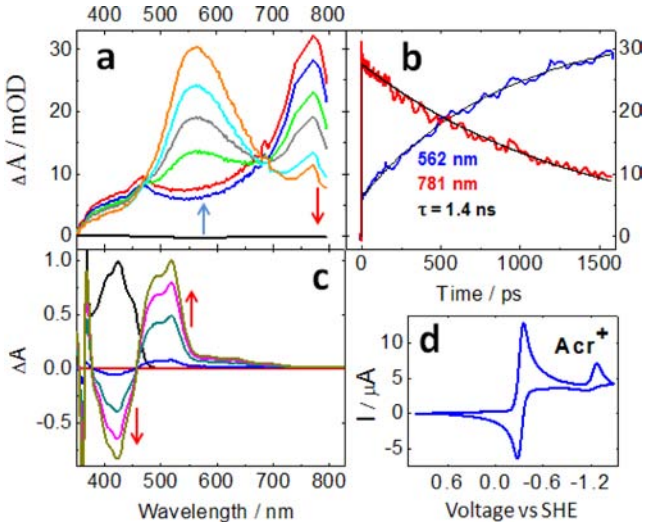

Figure 1. (a) Femtosecond TA spectra at time delays of −4.5 ps (black), 0 ps (red), 11 ps (blue), 310 ps (green), 570 ps (gray), 1150 ps (aqua), and 1574 ps (orange). (b) Kinetics of 1 mM AcrOH in ACN (λ_{EX} = 310 nm). (c) UV−vis spectroelectrochemical spectra of 1 mM Acr^+ in ACN at −0.56 V vs SHE at time delays of 0 s (red), 7 s (blue), 14 s (light blue), 21 s (magenta), and 49 s (olive). The black curve is the UV−vis absorption spectrum of Acr^+. (d) Cyclic voltammogram of 3 mM Acr^+ in anaerobic ACN containing 0.1 M tetrabutylammonium perchlorate. E_{red} = −0.3 V vs SHE.

is assigned to the S_1 state of AcrOH. The decay of the S_1 state is accompanied by the growth of a new band at ~550 nm that does not decay within 1.5 ns (the time limit of fs TA detection). The excited-state behavior of AcrOH and AcrOMe in other aprotic solvents, such as benzene (Figure S3 and Table S3), is similar to that shown in Figure 1. If the excited-state heterolytic C−O bond cleavage occurred, the 550 nm signal could be assigned to the formation of either Acr^+ (nonadiabatic process) or Acr^{+}* (adiabatic process). However, comparison of the absorption spectra of Acr^+ (λ_{max} = 425 nm; Figure 1c) and Acr^{+}* (λ_{max} = 390 and 470 nm; Figure S4) to this 550 nm band shows that the heterolytic C−O bond cleavage does not occur from the S1 state of AcrOH. On the basis of previous literature,[7] this ~550 nm peak could be postulated to arise from the acridine radical ($Acr^{\bullet}$), which would be formed by homolytic C−O bond cleavage (AcrOR + $h\nu$ → $Acr^{\bullet}$ + $^{\bullet}$OR). The absorption spectrum of $Acr^{\bullet}$ was obtained by a one-electron reduction of Acr^+ (see the cyclic voltammogram in Figure 1d). The UV−vis spectroelectrochemical results shown in Figure 1c demonstrate that $Acr^{\bullet}$ absorbs at 500 nm, which matches well with the previously reported $Acr^{\bullet}$ spectrum obtained using chemical reduction.[19] Given the large mismatch between the 550 nm band obtained in the TA spectra and the $Acr^{\bullet}$ signature band, we conclude that homolytic C−O bond cleavage from AcrOH* does not occur. The experiments performed on the ns time scale show that the 550 nm transient is long-lived ($\tau_{550\,nm}$ = 277 ns; Figure S5) and readily quenched by molecular oxygen. Thus, this intermediate is assigned to the triplet excited (T_1) state of AcrOH. These results suggest that even though the homolytic bond cleavage is thermodynamically favorable (Figure S1) and previous reports on similar systems[7] demonstrate the formation of the homolytic products, the S_1 state of AcrOH does not undergo homolytic C−O bond breaking. This is possibly due to a competing deactivation channel of the S_1 state via ISC to form the T_1 state. Additionally, formation of the $Acr^{\bullet}$ absorbance at ~500 nm was not observed in the ns TA measurements, showing that homolytic C−O bond cleavage on the T_1 state surface does not lead to separated $Acr^{\bullet}$ and $^{\bullet}$OH radicals, even though the evaluated AcrOH T_1 energy is higher than the energy needed for the C−O bond homolysis (Figure S1). A possible scenario that can explain this absence of observable homolytic products is one in which a conical intersection between the T_1 and S_0 states exists along the C−O bond coordinate. Since the T_1 lifetime of AcrOH (277 ns; Figure S5e) is shorter than the T_1 lifetimes of most organic compounds (usually in the μs to ms range[20]), it is possible that such a mechanism operates in this case. Indeed, DFT calculations suggested that homolytic C−O bond cleavage in the T_1 state occurs at a C−O bond distance of 1.8 Å. This triplet transition state would lead to a pair of separated radicals at a distance of 3.0 Å. However, along the C−O distance, the ground-state singlet surface and the triplet surface cross each other at a separation of 2.8 Å. Thus, we suggest that homolytic C−O bond cleavage in the triplet state leads to a conical intersection between the S_0 and T_1 states, resulting in the recovery of AcrOH in the ground state (see Table S2 and Figures S8−S10).

On the other hand, the behavior of AcrOH in protic solvents is different (Figure 2). The initially formed S_1 state decays within 108 ps to generate a product that absorbs at 425 nm. This product is assigned to Acr^+ by comparison to the ground-state absorption spectrum (Figure 2a inset). The protic solvation clearly has a strong effect on the energetics of the heterolysis, as schematized in Figure S1. As previously discussed by Steen,[21] the protic solvation stabilizes $^{-}$OH by promoting the migration of the negative charge along the hydrogen-bonded solvent network. The formation of Acr^+ occurs without any observable intermediate steps. To be specific, the formation of the intermediate Acr^{+}* via adiabatic heterolytic bond breaking along the S_1 surface of AcrOH was not observed in the TA spectra. The steady-state emission measurements also confirmed that Acr^{+}* is not formed as an intermediate during heterolytic bond cleavage (Figures S2 and S6), since no Acr^{+}* emission (450 to 650 nm) was observed in the emission measurements of AcrOH or AcrOMe in ACN or water.

The TA experiments on the ns time scale showed that the Acr^+ signal at 425 nm is long-lived, and no signal decay was observed within 100 μs (Figure 2d). The long-lived charge

dx.doi.org/10.1021/ja3031888 | J. Am. Chem. Soc. 2012, 134, 11301−11303

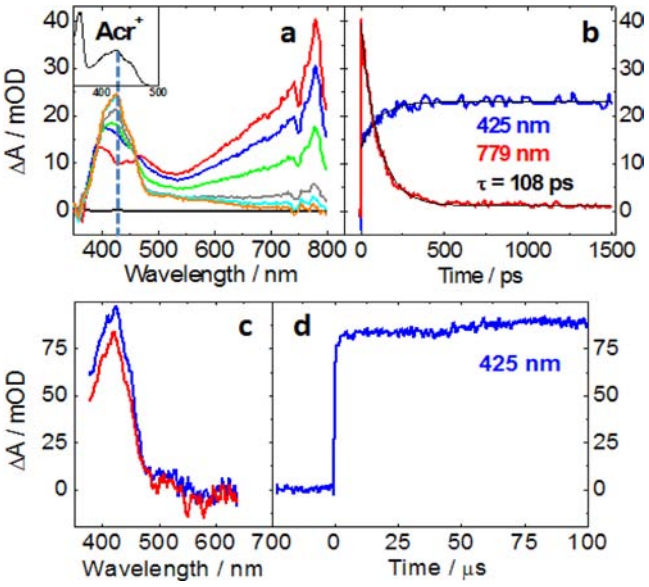

Figure 2. (a) Femtosecond TA spectra at time delays of −6.3 ps (black), 0 ps (red), 30 ps (blue), 80 ps (green), 200 ps (gray), 400 ps (aqua), and 1487 ps (orange). The inset shows the UV−vis absorption spectrum of Acr^+. (b) Kinetics of 1 mM AcrOH in MeOH (λ_{EX} = 310 nm). (c) Nanosecond TA spectra at time delays of 60 ns (red) and 510 ns (blue). (d) Kinetics of 0.17 mM AcrOH in O_2-saturated MeOH (λ_{EX} = 266 nm).

separation is most probably due to the high stability of the fully aromatic Acr^+ ion that is formed upon heterolysis. For example, a previous study showed an increase in the recombination lifetimes for more stable cations formed upon heterolysis.[9] The observed long lifetime of Acr^+ is a very encouraging result, since it demonstrates that the ^-OH generated in the photochemical process can be utilized to drive pOH jump experiments. Similar behavior was observed for AcrOMe; however, some differences are also worth mentioning. In the fs TA spectra of AcrOMe in MeOH (Figure S7), most of the AcrOMe was converted to Acr^+ after the laser flash, though there was still some generation of the T_1 state of AcrOMe (540 nm). These results reflect the fact that ISC is faster for AcrOMe. Comparison of the lifetime of the C−OH bond cleavage (108 ps) and the C−OMe bond cleavage (83 ps) shows that the C−OMe bond is weaker than the C−OH bond in MeOH. This conclusion is further supported by the known bond strengths of $PhCH_2$−OH and $PhCH_2$−OMe (78 and 68−70 kcal/mol, respectively).[8] The lower bond energy of C−OMe also reflects the different reactivities of AcrOH and AcrOMe in aprotic solvents: while AcrOH does not generate Acr^+ in aprotic solvents, the TA spectra of AcrOMe in ACN (Figures S3 and S5) show the formation of Acr^+ from the singlet excited state.

In conclusion, photochemical excitation of AcrOH has been shown to result solely in heterolytic cleavage in protic solvents. Since the heterolysis is fast (108 ps) and followed by slow recombination of the ions (time scale of hours[14]), the acridine derivatives such as AcrOH show promise for use in producing fast, long-lived pOH jumps.

■ ASSOCIATED CONTENT

Ⓢ Supporting Information

Synthesis, TA laser setup, computational methods, and additional fs and ns TA results. This material is available free of charge via the Internet at http://pubs.acs.org.

■ AUTHOR INFORMATION

Corresponding Author

kglusac@bgsu.edu

Notes

The authors declare no competing financial interest.

■ ACKNOWLEDGMENTS

This work was supported by BGSU, the National Science Foundation (CHE-1055397 CAREER Award to K.D.G. and CHE-0743258 to C.M.H.), the Ohio Supercomputer Center, and Delta Electronics Foundation (Delta Fellowship to D.Z.). We thank Felix N. Castellano (BGSU) for help with spectroelectrochemistry measurements.

■ REFERENCES

(1) Tolbert, L. M.; Solntsev, K. M. *Acc. Chem. Res.* **2002**, *35*, 19−27.
(2) Solntsev, K. M.; Clower, C. E.; Tolbert, L. M.; Huppert, D. *J. Am. Chem. Soc.* **2005**, *127*, 8534−8544.
(3) Ma, C.; Steinmetz, M. G.; Kopatz, E. J.; Rathore, R. *Tetrahedron Lett.* **2005**, *46*, 1045−1048.
(4) Shi, Z.; Peng, P.; Strohecker, D.; Liao, Y. *J. Am. Chem. Soc.* **2011**, *133*, 14699−14703.
(5) Gaillard, E.; Fox, M. A.; Wan, P. *J. Am. Chem. Soc.* **1989**, *111*, 2180−2186.
(6) McClelland, R. A.; Mathivanan, N.; Steenken, S. *J. Am. Chem. Soc.* **1990**, *112*, 4857−4861.
(7) Minto, R. E.; Das, P. K. *J. Am. Chem. Soc.* **1989**, *111*, 8858−8866.
(8) Manring, L. E.; Peters, K. S. *J. Phys. Chem.* **1984**, *88*, 3516−3520.
(9) Irie, M. *J. Am. Chem. Soc.* **1983**, *105*, 2078−2079.
(10) Wan, P.; Krogh, E. *J. Am. Chem. Soc.* **1989**, *111*, 4887−4895.
(11) Eom, K.; Jung, H.; Lee, G.; Park, J.; Nam, K.; Lee, S. W.; Yoon, D. S.; Yangad, J.; Kwon, T. *Chem. Commun.* **2012**, *48*, 955−957.
(12) Liu, H.; Xu, Y.; Li, F.; Yang, Y.; Wang, W.; Song, Y.; Liu, D. *Angew. Chem., Int. Ed.* **2007**, *46*, 2515−2517.
(13) Carvalho, C. P.; Uzunova, V. D.; Silva, J. P. D.; Nau, W. M.; Pischel, U. *Chem. Commun.* **2011**, *47*, 8793−8795.
(14) Ackmann, A. J.; Fréchet, J. M. J. *Chem. Commun.* **1996**, 605−606.
(15) Förster, T. *Z. Elektrochem.* **1950**, *54*, 42−46.
(16) Bunting, J. W.; Vivian, S. F. C.; Abhyankar, S. B.; Goda, Y. *Can. J. Chem.* **1984**, *62*, 351−354.
(17) Zhou, D.; Mirzakulova, E.; Khatmullin, R.; Schapiro, I.; Olivucci, M.; Glusac, K. D. *J. Phys. Chem. B* **2011**, *115*, 7136−7143.
(18) Sichula, V.; Kucheryavy, P.; Khatmullin, R.; Hu, Y.; Mirzakulova, E.; Vyas, S.; Manzer, S. F.; Hadad, C. M.; Glusac, K. D. *J. Phys. Chem. A* **2010**, *114*, 12138−12147.
(19) Ohkubo, K.; Suga, K.; Morikawa, K.; Fukuzumi, S. *J. Am. Chem. Soc.* **2003**, *125*, 12850−12859.
(20) Montalti, M.; Credi, A.; Prodi, L.; Gandolfi, M. T. In *Handbook of Photochemistry*; 3rd ed.; CRC Press: Boca Raton, FL, 2006; pp 83−156.
(21) Gurzadyan, G. G.; Steenken, S. *Chem.—Eur. J.* **2001**, *7*, 1808−1815.